Chloride transport in functionally active phagosomes isolated from Human neutrophils

Martha L. Aiken[a,1], **Richard G. Painter**[a], **Yun Zhou**[a], and **Guoshun Wang**[a,b,c,*]

[a]Department of Microbiology, Louisiana State University Health Sciences Center, New Orleans, LA 70112, USA

[b]Department of Genetics, Louisiana State University Health Sciences Center, New Orleans, LA 70112, USA

[c]Department of Medicine, Louisiana State University Health Sciences Center, New Orleans, LA 70112, USA

Abstract

Chloride anion is critical for hypochlorous acid (HOCl) production and microbial killing in neutrophil phagosomes. However, the molecular mechanism by which this anion is transported to the organelle is poorly understood. In this report, membrane-enclosed and functionally active phagosomes were isolated from human neutrophils by using opsonized paramagnetic latex microspheres and a rapid magnetic separation method. The phagosomes recovered were highly enriched for specific protein markers associated with this organelle such as lysosomal-associated membrane protein-1, myeloperoxidase (MPO), lactoferrin, and NADPH oxidase. When FITC–dextran was included in the phagocytosis medium, the majority of the isolated phagosomes retained the fluorescent label after isolation, indicative of intact membrane structure. Flow cytometric measurement of acridine orange, a fluorescent pH indicator, in the purified phagosomes demonstrated that the organelle in its isolated state was capable of transporting protons to the phagosomal lumen via the vacuolar-type ATPase proton pump (V-ATPase). When NADPH was supplied, the isolated phagosomes constitutively oxidized dihydrorhodamine 123, indicating their ability to produce hydrogen peroxide. The preparations also showed a robust production of HOCl within the phagosomal lumen when assayed with the HOCl-specific fluorescent probe R19-S by flow cytometry. MPO-mediated iodination of the proteins covalently conjugated to the phagocytosed beads was quantitatively measured. Phagosomal uptake of iodide and protein iodination were significantly blocked by chloride channel inhibitors, including CFTRinh-172 and NPPB. Further experiments determined that the V-ATPase-driving proton flux into the isolated phagosomes required chloride cotransport, and the cAMP-activated CFTR chloride channel was a major contributor to the chloride transport. Taken together, the data suggest that the phagosomal preparation described herein retains ion transport properties, and multiple chloride channels including CFTR are responsible for chloride supply to neutrophil phagosomes.

Keywords

Neutrophils; Phagosomes; V-ATPase; Chloride transporter; CFTR; Hypochlorous acid; Free radicals

[*]Corresponding author at: Department of Microbiology, Louisiana State University Health Sciences Center, New Orleans, LA 70112, USA. Fax: +1 504 568 8500. gwang@lsuhsc.edu. .
[1]Deceased.

Introduction

Neutrophils play an essential role in innate immunity, as they constitute the first line of defense against invading microorganisms. To limit collateral damage to surrounding cells or tissues and to enhance their microbicidal efficacy, neutrophils internalize foreign organisms into a specially formed organelle, referred to as the phagosome [1–3]. After containment, the microorganisms are assaulted and killed by toxic agents introduced by de novo synthesis within the organelle or acquired by fusion with storage gransules or vesicles [4–7].

Neutrophil phagosomes are a dynamic organelle. Electrons generated by the NADPH oxidase are translocated to the phagosomal lumen to reduce oxygen to superoxide anion (O_2^-). O_2^- is then dismutated to hydrogen peroxide (H_2O_2), which is further converted to hypochlorous acid (HOCl) by myeloperoxidase (MPO)[1] in the presence of chloride [8–10]. Thus, chloride availability to neutrophil phagosomes is critical to their function. Interestingly, resting neutrophils have an exceptionally high intracellular chloride level (80– 100 mM) [11,12]. When stimulated with serum-opsonized particles, the cells secrete a considerable amount of chloride to their phagosomes and extracellular space, which decreases the intracellular chloride levels by ~50% [12]. Notably, ionic and redox homeostasis in phagosomes is pivotal to their function. When translocated to the phagosomal lumen, the inward flow of electrons inevitably depolarizes the membrane, which, if not overcome, would otherwise inhibit the NADPH oxidase activity [13,14]. Therefore, efficient charge compensation mechanisms are needed to counteract the depolarization. One mechanism is to transport cations to the phagosomal lumen. Mounting evidence has indicated that protons are the major cation to countervail the inwardly transferred electrons, which is largely mediated by voltage-gated proton channels [13,14]. Inhibition of the proton channel by Zn^{2+} or other polyvalent metal cations significantly affects the oxidase activity by preventing charge compensation [15–18]. Moreover, neutrophils with ablated Hv1 proton channels substantially reduce their NADPH oxidase function by 30–75% [14,19–22]. However, deletion of Hv1 cannot completely abolish oxidant production, implying that other charge compensation mechanisms may coexist. Blocking the K^+/Cl^- cotransporter has been reported to affect the NADPH oxidase activity [23]. The electrogenic V-ATPase can actively pump protons inwardly [24,25]. Moreover, extrusion of anions, such as chloride, from the phagosomal lumen has also been proposed to offset the phagosomal depolarization [26]. However, this hypothesis is seemingly contradictory to the actual need for chloride in phagosomes for HOCl production. Thus, chloride movement across the phagosomal membrane and the molecules responsible for the action require experimental validation.

In this report, we obtained structurally intact and functionally active phagosomes from neutrophils using opsonized paramagnetic micrometer-sized particles. The preparations were suitable for ion transport studies when used in conjunction with flow cytometry. Experimental data have revealed that proton influx into the phagosomal lumen via V-ATPase is facilitated by chloride inward transport via multiple chloride channels, including CFTR. The results imply that the identified proton–chloride cotransport mechanism may be involved in phagosomal chloride acquisition and contribute to the overall ionic homeostasis of the organelle.

Materials and methods

Neutrophil isolation

Buffy coat preparations were obtained from normal volunteer donors or purchased from the Ochsner Clinic Foundation Blood Bank (New Orleans, LA, USA). The protocol used in this

study was approved by the LSU HSC IRB committee. The buffy coat fraction was gently mixed 1:1 (v/v) with 3% Dextran 400 (Sigma–Aldrich) in phosphate-buffered saline (PBS) without calcium or magnesium. The majority of the red cells were removed by sedimentation at $1g$ at 37 °C for 30 min. The resulting supernatant was subjected to fractionation by centrifugation through Ficoll–Hypaque (Histopaque; Sigma–Aldrich) at $800g$ for 30 min with slow acceleration and no brake at 23 °C. The plasma and mononuclear cell layer was aspirated off and discarded. The remaining pellet containing granulocytes and residual red blood cells was resuspended in PBS. Endotoxin-free water was added for 90 s to lyse the remaining red blood cells followed by the addition of a $10\times$ PBS stock to restore osmolarity to the normal level. Neutrophils were recovered by centrifugation and resuspended in Ringer's solution (122 mM NaCl, 1.2 mM $MgCl_2$, 1.2 mM $CaCl_2$, 2.4 mM K_2HPO_4, 0.6 mM KH_2PO_4, 20 mM Hepes, pH 7.3, and 10 mM dextrose) at 1×10^7 cells/ml.

Preparation of opsonized paramagnetic beads for phagocytosis

One-micrometer-size Dynabeads MyOne paramagnetic polystyrene carboxylated microspheres (Invitrogen) were washed twice with 25 mM 2-(N-morpholino)ethanesulfonic acid (Mes; pH 6.0) buffer by magnetic separation and resuspended to the original stock concentration in the same buffer. The particle-associated carboxyl groups were activated with fresh 1-ethyl-3-(3-dimethylaminopropyl)carbodiimide and N-hydroxysuccinimide (12.5 mg/ml each) for 30 min according to the manufacturer's instructions. After two washes with ice-cold Mes buffer, the beads were resuspended in an equal volume of 1% (w/v) bovine serum albumin (BSA) in the same buffer for 2 h at 4 °C with rotation. The beads were then washed three times with PBS by magnetic separation, followed by coating with rabbit anti-BSA antiserum (1:10) overnight with rotation. After three washes, the beads were stored at 4 °C in PBS containing 0.02% sodium azide. Just before use, the beads were incubated with an equal volume of fresh human male AB serum for 30 min at 37 °C to opsonize the beads with C3b. After one wash with PBS, the beads were resuspended and placed on ice until use.

Isolation of paramagnetic phagolysosomes (PM-PLS)

Neutrophils (1×10^7) were incubated at 37 °C for 20 min with the IgG–C3b-opsonized paramagnetic particles prepared as described above at a ratio of 5–10 per neutrophil. After ingestion, the cells were washed twice by centrifugation ($51g$) for 5 min at 4 °C to remove free particles. The brownish cell pellet containing ingested particles was resuspended to 5×10^7 cells/ml and treated with 5 mM DFP for 10 min on ice and then washed twice with PBS. The final pellet was resuspended to the same cell density in the chloride-rich relaxation buffer (100 mM KCl, 2 mM $MgCl_2$, 1.25 mM EGTA, 1 mM ATP, 20 mM Pipes, pH 7.2) containing a protease inhibitor cocktail and, where indicated, a phosphatase inhibitor cocktail (Sigma–Aldrich) and then subjected to nitrogen cavitation (400 psi) as described elsewhere [27]. The rationale of using the chloride-rich relaxation buffer with the physiological chloride level in resting neutrophils is to maintain the maximal chloride gradient across the phagosomal membrane. After lysis, the homogenate was centrifuged at $51g$ for 5 min to remove any remaining intact cells. The phagosomes were harvested by magnetic attraction for 1 min. The supernatant was poured off and the remaining magnetic phagosomes were similarly washed six or seven times with homogenization buffer and finally resuspended to a volume of buffer equal to that of the starting homogenate.

Characterization of phagosomes by flow cytometry

Freshly isolated PM-PLS samples were assayed for lysosomal-associated membrane protein-1 (LAMP-1) antigen by incubating with Cy3-labeled rabbit anti-human LAMP-1 (1:50; Sigma–Aldrich) in PBS containing 2% normal goat serum. After 1 h, the PM-PLS

were washed twice with the aid of a magnet. Then, the PM-PLS were analyzed with a Becton–Dickinson Excalibur flow cytometer. The light-scatter discriminators were set to monitor the monomeric bead particles in each case.

Assessment of the membrane integrity of isolated PM-PLS

The percentage of sealed PM-PLS was evaluated by FITC–dextran retention assay. PM-PLS were labeled with FITC–dextran (Sigma–Aldrich; 40 kDa) by including 0.5 mg/ml FITC–dextran in the medium during particle phagocytosis. After cell lysis and magnetic isolation, the phagosomes were immunostained with Cy3-labeled anti-LAMP-1 antibody. The percentage of FITC-positive/LAMP-1-positive phagosomes was determined by flow cytometry. Preliminary stability studies indicated that the retained FITC–dextran levels were stable for at least 4 h but had diminished by 50% after overnight storage at 4 °C. Therefore, subsequent experiments requiring sealed preparations were performed within 4 h of preparation.

Lactate dehydrogenase (LDH) assay

LDH was assayed spectrophotometrically using a kit obtained from Sigma–Aldrich in the presence of the nonionic detergent provided with the kit.

Immunoblotting for phagosome-associated marker proteins

Isolated phagosomes or all other neutrophil components were applied to 7.5% Laemmli gels as previously described [28]. Equal cell equivalents (3.35×10^5) were loaded onto each lane so that the relative enrichment of each marker could be evaluated. The primary antibodies were rabbit polyclonal antibodies (Sigma–Aldrich) specific for human lactoferrin (LF), LAMP-1, and MPO and used at 1:4000 dilution. The secondary antibody was goat anti-rabbit IgG horseradish peroxidase conjugate at 1:6000 dilution. After being washed, the membranes were developed with a chemiluminescence kit (Pierce). Quantitation of the detection level was performed directly on the chemiluminescent immunoblot using a Bio-Rad ChemDoc XRS chemiluminescence detector.

NADPH oxidase activity in isolated PM-PLS

Superoxide dismutase-sensitive NADPH–cytochrome c reductase activity in cell homogenates and associated subcellular fractions was measured spectrophotometrically as indicated [29]. Activity was defined by measuring the reduction of cytochrome c (5 nmol in 1.0 ml) by monitoring the change in absorbance at 550 nm. The difference in A_{550} in the presence or absence of SOD (Sigma–Aldrich) over 20 min was obtained and the nanomoles of reduced cytochrome c were determined using an extinction coefficient of 21.1 nM^{-1} cm^{-1}.

In the experiments indicated, NADPH oxidase activity was measured by monitoring the oxidation of dihydrorhodamine 123 (DHR). Briefly, the isolated phagosomes were diluted into 0.8 ml of the relaxation buffer containing 5 μM dihydrorhodamine 123 (Invitrogen) and 1 mM ATP. The membrane-permeative, nonfluorescent DHR is oxidized (primarily by hydrogen peroxide generated by NADPH oxidase-generated superoxide dismutation) within the phagosome lumen to a green-fluorescent charged species that is trapped within the phagosome. After addition of the NADPH substrate, the fluorescent product can be conveniently measured with time by conventional flow cytometry and the linear rate of production estimated. No oxidation of DHR was noted in the absence of NADPH.

Measurement of proton transport in isolated PM-PLS

The Percoll-gradient-purified neutrophils were resuspended in Ringer's solution and the opsonized magnetic particles were phagocytosed. Then, the cells were lysed in the relaxation buffer containing protease inhibitors. After nitrogen cavitation, the phagosomes were separated. Acidification of the isolated phagosomes was measured by monitoring the fluorescence of acridine orange (4 μM) by flow cytometry. This dye rapidly partitions into acidic organelles and is highly fluorescent within that environment [30]. The FL2 flow cytometry channel was gated on the 1.0 μm monomer population detected by combined forward and 90° light scatter and the mean fluorescence channel number was measured at 30-s intervals. The initial time-point fluorescence value was subtracted from that of the subsequent time points to obtain the total change in fluorescence of the preparation.

HOCl production in isolated phagosomes

Phagosomes were isolated, washed, and resuspended in the relaxation buffer with various concentrations of chloride, as indicated, to examine the effect of chloride on HOCl production within the isolated phagosomes. The isolated phagosomes, mixed with NADPH (200 μM) and PKA (10 U/ml) in the presence or absence of diphenylene iodonium (DPI; 10 μM) or ABAH (200 μM), were incubated at 37 °C for 30 min, followed by addition of 10 μM R19-S (FutureChem Co., Seoul, Republic of Korea) for 10 more minutes. Then, the samples were fixed with 4% paraformaldehyde for flow cytometry analysis.

Uptake of radioactive iodide by isolated phagosomes and iodination of bead-bound proteins

Freshly magnet-isolated phagosomes (0.1 ml) were mixed with 0.1 ml of the chloride-free relaxation buffer (100 mM potassium gluconate, 2 mM $MgCl_2$, 1.25 mM EGTA, 1 mM ATP, 20 mM Pipes, pH 7.2) containing the test ion channel inhibitors or MPO inhibitor at concentrations indicated in the text or with the dimethyl sulfoxide vehicle as a control. The rationale for using chloride-free relaxation buffer here was to avoid chloride competition with iodine for channels. D-Methionine (10 mM), a membrane-impermeative and nontransportable amino acid, was added to scavenge any hypoiodous acid generated by extraphagosomal MPO. The reaction was started by adding freshly diluted H_2O_2 (0.5 mM) and ^{125}I (10 μCi). The reaction was terminated 30 s later as the initial time point or 30 min later by adding 1 ml of lysis buffer containing 100 mM KI, 5 mM sodium azide, potassium metabisulfite, and 0.1% Triton X-100. This buffer served to block further MPO action and lysed the phagosomal membrane to release any trapped free iodide and non-bead-associated proteins that might be radiolabeled. The radioactive labeled paramagnetic beads were then collected by filtration onto 0.45-μm HA Millipore nitrocellulose 25-mm filters and washed four times with the same buffer. The bead-coupled radioactivity was assessed by liquid scintillation in 10 ml of Cytoscint aqueous scintillation fluid. Preliminary experiments showed that the uptake of iodide was time-, MPO-, and hydrogen peroxide-dependent. None of the ion channel inhibitors used in the assay had any effect on MPO activity as assessed by oxidation of 3,3′,5,5′-tetramethylbenzinide. The ABAH-inhibitable iodination of each group was compared with that of the nontreatment control.

Results

Phagosome purification and characterization

Dynabead MyOne 1-μm paramagnetic particles were fed to neutrophils after opsonization with IgG and C3b, as described under Materials and methods. After 20 min at 37 °C the cells were washed by low-speed centrifugation at 4 °C to remove free particles and resuspended in the relaxation buffer containing ATP and a cocktail of protease inhibitors

and, where indicated, phosphatase inhibitors. After nitrogen cavitation, the magnetic microspheres were harvested using a magnet and washed multiple times with and finally resuspended in the ice-cold relaxation buffer. This protocol was rapid, taking less than 1 h from the time of cell lysis to completion. The procedure was also mild in that no osmotically harsh gradients, such as sucrose, were needed to further purify the phagosomes.

To examine the integrity and quality of the prepared phagosomes, we performed flow cytometric analysis. Fig. 1A shows the forward- and side-scatter profiles of the PM-PLS. As indicated, a large population of the phagosomes contained 1-μm-sized monomeric beads, as well as polymeric forms of phagosomes. Hereafter, we focused our flow cytometric analyses on the monomeric phagosome population. To examine the intactness of the phagosomal membrane, we assessed the ability of the isolated phagosomes to retain the FITC–dextran that was taken up from the fluid-phase medium during phagocytosis. Fig. 1C shows that ~59% of the monomeric bead population retained FITC–dextran, whereas the negative control (Fig. 1B) without addition of FITC–dextran to the medium was not stained. Further, the beads-alone control or the detergent-treated phagosome control had no fluorescence associated with the gated monomeric population (data not shown), suggesting that the FITC–dextran was enclosed only in the membrane-bound, intact phagosomes. The Cy3–anti-LAMP-1 staining indicated that ~92% of the isolated phagosomes was positive for LAMP-1 (Fig. 1D). About 48% of the LAMP-1-positive monomeric phagosomes were positive for FITC–dextran and 3.4% of phagosomes were LAMP-1-negative but FITC-positive, implying that they were immature phagosomes. These data suggest that more than half of the monomeric phagosomes were sealed.

Next, we assessed the purity of the isolated phagosomes by monitoring the recovery of various subcellular markers. Measurement of the cytosolic marker enzyme lactate dehydrogenase suggested that ~99% of the LDH activity was retained in the non-PM-PLS fraction (Table 1). Immunoblot and quantitative chemiluminescence analyses of the purified phagosomes and the nonmagnetic remaining fractions showed a significant enrichment, relative to the total recovered protein, for LAMP-1, MPO, and LF, of 13-, 4.6-, and 7.6-fold, respectively (Table 1). We also monitored particle recovery at each step and found that at least 90–95% of the particles phagocytosed were recovered in the final phagosomal preparation.

We further examined if the NADPH oxidase complex, which is known to be assembled on the phagosomal membrane during phagocytosis, survived the isolation procedure and remained functional. NADPH oxidase activity, as defined by the presence of a NADPH-dependent, SOD-inhibitable cytochrome *c* reductase activity, was detected in the phagosome fraction and accounted for 43% of the total recovered enzyme activity (Fig. 2A). The PM-PLS fraction was enriched for the NADPH oxidase by 12-fold over that present in the starting cell extract but was only 1.2-fold enriched in the non-PM-PLS fraction. This compares favorably with the reported ~6-fold enrichment for latex phagosomes isolated by ultracentrifugation on sucrose density gradients [29]. To confirm if the NADPH oxidase was constitutively active, we assayed the purified phagosomes in the presence of NADPH substrate for their ability to oxidize and thereby trap and accumulate oxidized dihydrorhodamine 123 by flow cytometry. As Fig. 2B indicates, the oxidation of this fluorescent probe was linear over the time course of the experiment and was inhibited by DPI, a potent and specific NADPH oxidase inhibitor. These data indicate that the magnetic isolation protocol described here gave rise to a good yield of sealed phagosomes with high enrichment of marker proteins and enzyme activities known to be associated with mature and functional phagosomes.

V-ATPase transports protons in isolated phagosomes without activation of NADPH oxidase

To examine whether the isolated phagosomes retained a functional V-ATPase proton pump, we resuspended the obtained PM-PLS in the relaxation buffer containing 1 mM ATP and 4 μM acridine orange (AO). AO, a weak-base dye, fluoresces in acidic subcellular compartments and has been used to detect acidification in isolated lysosomes, endocytotic granules, and synaptic vesicles, as well as whole cells [31–33]. Any acidification within the lumen of the phagosomes would result in an increase in AO fluorescence within the phagosome population when measured by flow cytometry. As shown in Fig. 3, when valinomycin, a potassium ionophore, was added to neutralize the membrane potential caused by any existing K^+ gradient [30], a rapid acidification ensued. Addition of nigericin, an ionophore that exchanges K^+ and H^+, returned the AO fluorescence to the initial baseline level, indicating that the increase in fluorescence caused by ATP and valinomycin was due to acidification within the phagosomal lumen. Preincubation of the phagosomes with concanamycin A blocked the response, showing that the pH changes were primarily due to the action of the V-ATPase. In this experiment, NADPH was not added exogenously and was not present in the system. Thus, the NADPH oxidase was not activated. Therefore, the V-ATPase must function independent of NADPH oxidase activity. This result from our cell-free system is in agreement with Grinstein and co-workers, who have shown V-ATPase-mediated phagosomal acidification in intact neutrophils when the NADPH oxidase is inhibited by DPI [25].

Chloride-dependent HOCl production in the isolated phagosomes

To determine if the isolated phagosomes were able to produce HOCl, we measured the oxidation of R19-S, a HOCl-specific fluorescent probe, by flow cytometry. R19-S in its natural state does not fluoresce. However, HOCl oxidation renders it fluorescent [34]. As shown in Fig. 4, the fluorescence of the HOCl sensor in the isolated phagosomes increased as the medium chloride level escalated (Fig. 4C–H), indicating a chloride-dependent production of HOCl. Such an oxidation reached saturation after 67 mM medium chloride. Further, when DPI or ABAH or a combination of both was used, the fluorescence diminished (Fig. 4K–P), validating that HOCl production was dependent on the NADPH oxidase and MPO. Thus, the isolated phagosomes had active MPO and NADPH oxidase and were competent to generate HOCl from chloride.

Functional chloride channels permit MPO-mediated halogenation in the isolated phagosomes

Physiologically chloride is the most abundant anion. However, MPO has the ability to catalyze oxidation of any present halides, such as chloride, bromide, and iodide, into hypohalous acid [35,36]. Moreover, chloride channels transport not only chloride but also the other halides [35,37]. Taking advantage of these properties, we quantitatively measured the chloride channel function in the isolated phagosomes by radioactive iodination assay. The isolated PM-PLS were treated with various chloride channel inhibitors or MPO inhibitor in the presence of hydrogen peroxide (0.5 mM) and ^{125}I (10 μCi). The radioactivity covalently coupled to the bead-associated proteins was determined after detergent extraction and collection of the bead particles on nitrocellulose membrane filters. D-Methionine, a membrane-impermeative and nontransportable amino acid, was added to scavenge any MPO-generated hypoiodous acid present in the extraphagosomal medium. A cocktail of protease and phosphatase inhibitors was included in the cavitation medium to ensure that the native protein structures and maximal phosphorylation of critical ion channels were maintained through the phagosomal isolation procedure. As shown in Fig. 5, the isolated phagosomes were able to transport radioactive iodide to the phagosomal lumen and to produce hypoiodous acid, which iodinated the bead-conjugated proteins. The ABAH-

inhibitable iodination of each group was compared to that of the nontreatment control. CFTRinh-172, a highly potent and specific inhibitor for CFTR chloride channel [38], significantly inhibited the iodide transport and thus iodination of the bead-conjugated proteins by ~47%. The broad-spectrum anion channel inhibitor NPPB inhibited the iodination by ~72%. Combination of the two inhibitors did not have any additive effect. These data suggest that more than one chloride channel is probably involved in the halide transport to the phagosomal lumen. Notably, the CFTR channel accounted for about half of the iodide intake by the phagosomes, which is in accord with our previous measurement of iodide intake in intact neutrophils [39].

Proton transport by V-ATPase Is associated with chloride transport in the isolated phagosomes

Proton transport in coated vesicles was reported to require cotransport of chloride [40]. We sought to determine the role of V-ATPase in neutrophil phagosomal chloride movement. Toward this end, 4 μM AO was added to the isolated phagosomes. Then, the mixture was subjected to flow cytometric measurement of AO fluorescence. Changes in the fluorescence intensity seen in response to various treatments are displayed in Fig. 6. Without activation of V-ATPase in the no-ATP control (Fig. 6) no phagosomal acidification occurred. When ATP and the cAMP-stimulatory analogue (Sp-cAMPS) were applied to the system, the phagosomal lumen was acidified rapidly, exemplified by the increase in the AO fluorescence (Fig. 6). However, when ATP and the cAMP-inhibitory analogue (Rp-cAMPS) were added (Fig. 6), the acidification was inhibited to ~46% of the maximal value. When a CFTR-specific inhibitor (CFTRinh-172 or Ap5A) was included, the responses were reduced to ~54% of the maximal value. In the absence of cAMP, the inhibitors did not show any effect (data not shown). It is known that the two CFTR inhibitors act through different mechanisms. CFTRinh-172 blocks the CFTR channel by pore occlusion from the cytosolic side of the phagosomal membrane [38], whereas Ap5A inhibits CFTR adenylate kinase activity to prevent the channel opening by interacting with the ATP binding domain of the regulatory region of CFTR [41]. Furthermore, CFTR is a cAMP-activated chloride channel. Thus, both the CFTR inhibitors and the cAMP-inhibitory analogue attenuated the phagosomal acidification, suggesting CFTR is a major channel in charge compensation associated with proton movement across the phagosomal membrane by the vacuolar H^+ pump. Moreover, NPPB inhibited the phagosomal acidification to ~52% (Fig. 6). Therefore, there existed a mechanism in which the V-ATPase-mediated proton translocation was associated with chloride channel-mediated chloride transport in neutrophil phagosomes.

To confirm the above finding that chloride limits V-ATPase-mediated proton translocation, we sought to examine acidification of the isolated phagosomes in the presence or absence of chloride and in the presence or absence of ROS production. Flow cytometric analysis showed that the cAMP-induced change in phagosomal AO fluorescence was blunted if no chloride was provided to the reconstituted phagosome system (Fig. 7A). There was no significant difference of the phagosomal pH regardless of oxidant production under the no-chloride condition. However, when chloride was available and ROS production was not activated, the phagosomes were acidified rapidly upon cAMP activation of chloride transport. In contrast, when chloride was available and ROS was produced, the phagosomes were not able to acidify (Fig. 7B). From these data we conclude that H^+ translocation by V-ATPase requires chloride to proceed efficiently. ROS, produced by the activated NADPH oxidase and MPO, suppressed the phagosomal acidification, presumably by consumption of H^+ and chloride to form HOCl or other oxidants, which may subsequently convert to nonionic products or escape from the phagosomes.

Discussion

Isolation of membrane-enclosed and functionally active phagosomes has been a challenge to the field. An ideal preparation should have the following properties: (a) the phagosomal membrane must be in a sealed state after purification, (b) the procedure must be mild and rapid so as to minimize loss of essential associated protein components by proteolysis, (c) the yield should be high, and (d) the preparations should be suitable for downstream analysis. To our best knowledge, there have been no reports of measurements of phagosomal ion transport in its isolated state, even though reports are available for other isolated subcellular organelles such as membrane vesicles and endosomes [30,42,43]. Here, we used the magnet-attraction method for rapid isolation of functional phagosomes from neutrophils that were suitable for assessing ion transport in vitro. The use of magnetic particles in the form of bacteria coated with submicrometer-sized magnetic particles to isolate phagosomes was previously reported [44,45]. However, there was no functional assessment of the isolates in those studies. The current report presents the first case of examining phagosomal ion dynamics in its isolated state.

An unresolved issue in neutrophil biology is how the negatively charged chloride ion enters the phagosomal lumen where it is utilized to generate hypochlorous acid. Nearly 90% of the oxygen consumed during the respiratory burst of neutrophils during phagocytosis is converted ultimately to hypochlorous acid [46], which is approximately 3–4 nmol O_2 molecules per minute per million cells [46,47]. Given this rate, any chloride ion entrapped within the phagosome during phagocytosis of extracellular medium would be consumed in less than a minute [46]. Thus, a continuous source of chloride is necessary after internalization of the phagosome to account for continued HOCl production. According to the HOCl chemical synthesis formula ($H_2O_2 + Cl^- + H^+ \xrightarrow{MPO} HOCl + H_2O$), an equivalent amount of chloride must be transported into the phagosome to account for this chemical synthesis, which allows generation of sufficient concentration of HOCl in the organelle for microbicidal action [48]. Our laboratory has previously measured the rate of chloride uptake in phagosomes of intact neutrophils and found it to be on the order of 0.31 mM/s under the condition of active NADPH oxidase and inhibited MPO. The luminal concentration of chloride is ~70 mM under steady-state conditions [49], which is higher than the measured cytosolic level of 40–50 mM chloride in stimulated neutrophils [49,50]. This counterintuitive finding implies that a driving force must exist to permit chloride accumulation on the luminal side of the phagosome membrane. To achieve such chloride counterflow, energy must be expended in some form to favor chloride flow from the cytosol to the phagosomes. Activation of the NADPH oxidase would be expected to make the phagosome interior highly negatively charged (depolarized), which theoretically hampers any anion entry. The Zn^{2+}-inhibitable proton channel or voltage-gated proton channel is reported to provide the bulk charge compensation needed for the respiratory burst in neutrophils [13]. Because of the passive transport property of the proton channel, it is believed that this mechanism cannot generate net positive charge in the phagosomal lumen that facilitates chloride anion influx to phagosomes. However, inactivation of the V-ATPase by concanamycin A reduces the phagosomal membrane potential in macrophages from a value of near +28 mV (lumen positive) to about +17 mV [51]. It is important to realize that these measurements were made about 7 min after particle phagocytosis so the NADPH oxidase should be operating at near steady-state levels. Thus, the net inside positive potential contributed by the V-ATPase (+11 mV) should help drive chloride ions into the phagosome. A potential differential of +11 mV maintained by the V-ATPase proton pump would result in a Nernst-driven redistribution of chloride such that if the cytosolic level was about 45 mM as phagocytosing or stimulated cells, a 69 mM phagosomal concentration would be predicted from electrogenic considerations alone. Assuming that a similar situation occurs in neutrophils, the V-ATPase could in theory provide the potential energy via ATP hydrolysis

to maintain an electrically favorable environment to facilitate chloride entry into the phagosome. Our experimental data from analyzing the V-ATPase-mediated phagosomal acidification and chloride channel-mediated chloride transport clearly indicate the possible functional association of the two molecules. Based on the experimental data, we propose a model for chloride acquisition and charge balance in neutrophil phagosomes, as displayed in Fig. 8. Three important features of this model are noteworthy: (1) the NADPH oxidase and V-ATPase are the two chief electrogenic molecules. The two enzymes function independent of each other. The NADPH oxidase depolarizes the phagosomal membrane. Any significant changes in phagosomal membrane potential would be sensed and regulated by the voltage-gated proton and potassium channels. Protons and potassium ions are transported to the phagosomal lumen to balance the increase in negative charges, which constitutes the major charge compensation mechanism for relieving the NADPH oxidase-generated membrane depolarization. (2) The V-ATPase pump delivers protons to the phagosome independent of the NADPH oxidase. This charge movement would be balanced by anions such as chloride. (3) Even though some portion of chloride consumption is reversible, such as HOCl reaction with thiols and thioesters, a significant portion of chloride consumption is irreversible owing to HOCl escaping from the phagosomes or turning into nonionic chlorinated products at the phagosomes. Thus, a chloride gradient may be generated, which further favors chloride influx. Therefore, both electrical potential generated by V-ATPase and chemical potential derived from the chloride gradient drive chloride to accumulate in the phagosomes.

In this report, we measured iodide transport by an indirect method via monitoring MPO-mediated incorporation of radioactive iodide into bead-bound proteins. This assay included D-methionine in the extracellular medium to scavenge any hypoiodous acid production by nonintraphagosomal MPO. Halide channel activities were detected and able to be blocked by selected anion channel inhibitors such as NPPB and CFTRinh-172. These data conclusively showed that CFTR was a major player in the halide transport to phagosomal lumen, contributing ~50% of the total halide transport capacity. These results are consistent with our previous report using halide-specific fluorescent probes bound to zymosan particles, in which we found that phagosomal chloride or iodide transport into the phagosomes is reduced compared to normal when the cells are incubated with CFTR inhibitors or when neutrophils from CF patients are used [39,52]. Multiple chloride transporters have been identified in neutrophils, such as Ca^{2+}-activated chloride channels [53], ClC-3 (chloride channel-3) [54], the Na^+–K^+–$2Cl^-$ exchanger [11,55], the Cl^-–HCO_3^- exchanger [55], the swelling-induced chloride channels [56,57], and the PKA-activated CFTR chloride channel [52]. ClC-3 and CFTR have been found on neutrophil phagosomes [52,54]. At this point we do not know how many chloride channels are present in the phagosomes that might participate in chloride permeativity. The availability of these preparations should allow us to address this issue in future studies.

In summary, we have developed a method for the near-quantitative isolation of phagosomes from human neutrophils that is rapid and straightforward. The preparation is enriched with respect to phagosomal markers associated with mature phagosomes and retains critical enzymatic and ion transport properties and, therefore, should be useful for detailed in vitro analysis of the biochemical functioning of this important subcellular organelle. Using the purified phagosomes we have identified that multiple chloride channels contribute to halide permeativity. The CFTR channel accounts for about half of the halide acquisition. Further, the V-ATPase proton pump is capable of providing electrogenic energy for the accumulation of chloride in the phagosomal lumen where it would be needed for hypochlorous acid production for bacterial killing.

Acknowledgments

Abbreviations

|	
ABAH	4-aminobenzoic acid hydrazide
AO	acridine orange
CFTR	cystic fibrosis transmembrane conductance regulator
DFP	diisopropylfluoro-phosphate
DHR	dihydrorhodamine 123
Hepes	4-(2-hydroxyethyl)-1-piperazineethanesulfonic acid
LAMP-1	lysosomal-associated membrane protein-1
LDH	lactate dehydrogenase
LF	lactoferrin
MPO	myeloperoxidase
NPPB	5-nitro-2-(3-phenylpropylamino)benzoic acid
PKA	catalytic subunit of protein kinase A
PM-PLS	paramagnetic phagolysosomes
SOD	superoxide dismutase
V-ATPase	vacuolar-type ATPase proton pump
ClC-3	chloride channel-3
CFTRinh-172	5-[(4-carboxyphenyl)methylene]-2-thioxo-3-[(3-trifluoromethyl)phenyl-4-thiazolidinone
Sp-cAMPS	Sp-adenosine-3′,5′-cyclic monophosphorothioate
Rp-cAMPS	Rp-adenosine-3′,5′-cyclic monophosphorothioate
Ap5A	P1,P5-di(adenosine-5′) pentaphosphate

References

[1]. Klebanoff SJ. Myeloperoxidase: friend and foe. J. Leukocyte Biol. 2005; 77:598–625. [PubMed: 15689384]

[2]. Nauseef WM. How human neutrophils kill and degrade microbes: an integrated view. I mmunol. Rev. 2007; 219:88–102.

[3]. Flannagan RS, Cosio G, Grinstein S. Antimicrobial mechanisms of phagocytes and bacterial evasion strategies. Nat. Rev. Microbiol. 2009; 7:355–366. [PubMed: 19369951]

[4]. Lehrer RI, Ganz T, Selsted ME. Oxygen-independent bactericidal systems: mechanisms and disorders. Hematol. Oncol. Clin. North Am. 1988; 2:159–169. [PubMed: 3279018]

[5]. Hampton MB, Kettle AJ, Winterbourn CC. Inside the neutrophil phagosome: oxidants, myeloperoxidase, and bacterial killing. Blood. 1998; 92:3007–3017. [PubMed: 9787133]

[6]. Borregaard N, Cowland JB. Granules of the human neutrophilic polymorphonuclear leukocyte. Blood. 1997; 89:3503–3521. [PubMed: 9160655]

[7]. Ganz T, Selsted ME, Lehrer RI. Defensins. Eur. J. Haematol. 1990; 44:1–8. [PubMed: 2407547]

[8]. Klebanoff SJ. Myeloperoxidase–halide–hydrogen peroxide antibacterial system. J. Bacteriol. 1968; 95:2131–2138. [PubMed: 4970226]

[9]. Albrich JM, McCarthy CA, Hurst JK. Biological reactivity of hypochlorous acid: implications for microbicidal mechanisms of leukocyte myeloperoxidase. Proc. Natl. Acad. Sci. USA. 1981; 78:210–214. [PubMed: 6264434]

[10]. Hurst JK, Albrich JM, Green TR, Rosen H, Klebanoff S. Myeloperoxidase-dependent fluorescein chlorination by stimulated neutrophils. J. Biol. Chem. 1984; 259:4812–4821. [PubMed: 6325409]

[11]. Simchowitz L, De Weer P. Chloride movements in human neutrophils: diffusion, exchange, and active transport. J. Gen. Physiol. 1986; 88:167–194. [PubMed: 3746250]

[12]. Busetto S, Trevisan E, Decleva E, Dri P, Menegazzi R. Chloride movements in human neutrophils during phagocytosis: characterization and relationship to granule release. J. Immunol. 2007; 179:4110–4124. [PubMed: 17785850]

[13]. DeCoursey TE. Voltage-gated proton channels find their dream job managing the respiratory burst in phagocytes. Physiology (Bethesda). 2010; 25:27–40. [PubMed: 20134026]

[14]. Morgan D, Capasso M, Musset B, Cherny VV, Rios E, Dyer MJ, DeCoursey TE. Voltage-gated proton channels maintain pH in human neutrophils during phagocytosis. Proc. Natl. Acad. Sci. USA. 2009; 106:18022–18027. [PubMed: 19805063]

[15]. Henderson LM, Chappell JB, Jones OT. The superoxide-generating NADPH oxidase of human neutrophils is electrogenic and associated with an H+ channel. Biochem. J. 1987; 246:325–329. [PubMed: 2825632]

[16]. Femling JK, Cherny VV, Morgan D, Rada B, Davis AP, Czirjak G, Enyedi P, England SK, Moreland JG, Ligeti E, Nauseef WM, DeCoursey TE. The antibacterial activity of human neutrophils and eosinophils requires proton channels but not BK channels. J. Gen. Physiol. 2006; 127:659–672. [PubMed: 16702353]

[17]. DeCoursey TE, Morgan D, Cherny VV. The voltage dependence of NADPH oxidase reveals why phagocytes need proton channels. Nature. 2003; 422:531–534. [PubMed: 12673252]

[18]. Chvapil M, Stankova L, Bernhard DS, Weldy PL, Carlson EC, Campbell JB. Effect of zinc on peritoneal macrophages in vitro. Infect. Immun. 1977; 16:367–373. [PubMed: 873614]

[19]. El Chemaly A, Demaurex N. Do Hv1 proton channels regulate the ionic and redox homeostasis of phagosomes? Mol. Cell. Endocrinol. 2012; 353:82–87. [PubMed: 22056415]

[20]. El Chemaly A, Okochi Y, Sasaki M, Arnaudeau S, Okamura Y, Demaurex N. VSOP/Hv1 proton channels sustain calcium entry, neutrophil migration, and superoxide production by limiting cell depolarization and acidification. J. Exp. Med. 2010; 207:129–139. [PubMed: 20026664]

[21]. Ramsey IS, Ruchti E, Kaczmarek JS, Clapham DE. Hv1 proton channels are required for high-level NADPH oxidase-dependent superoxide production during the phagocyte respiratory burst. Proc. Natl. Acad. Sci. USA. 2009; 106:7642–7647. [PubMed: 19372380]

[22]. Musset B, Cherny VV, Morgan D, DeCoursey TE. The intimate and mysterious relationship between proton channels and NADPH oxidase. FEBS Lett. 2009; 583:7–12. [PubMed: 19084015]

[23]. Sun YT, Shieh CC, Delpire E, Shen MR. K^+-Cl^- cotransport mediates the bactericidal activity of neutrophils by regulating NADPH oxidase activation. J. Physiol. 2012; 590:3231–3243. [PubMed: 22526882]

[24]. Lukacs GL, Rotstein OD, Grinstein S. Phagosomal acidification is mediated by a vacuolar-type H(+)-ATPase in murine macrophages. J. Biol. Chem. 1990; 265:21099–21107. [PubMed: 2147429]

[25]. Jankowski A, Scott CC, Grinstein S. Determinants of the phagosomal pH in neutrophils. J. Biol. Chem. 2002; 277:6059–6066. [PubMed: 11744729]

[26]. Behe P, Segal AW. The function of the NADPH oxidase of phagocytes, and its relationship to other NOXs. Biochem. Soc. Trans. 2007; 35:1100–1103. [PubMed: 17956288]

[27]. Kjeldsen L, Sengelov H, Borregaard N. Subcellular fractionation of human neutrophils on Percoll density gradients. J. Immunol. Methods. 1999; 232:131–143. [PubMed: 10618515]

[28]. Gomez M, Raju SV, Viswanathan A, Painter RG, Bonvillain R, Byrne P, Nguyen DH, Bagby GJ, Kolls JK, Nelson S, Wang G. Ethanol upregulates glucocorticoid-induced leucine zipper expression and modulates cellular inflammatory responses in lung epithelial cells. J. Immunol. 2010; 184:5715–5722. [PubMed: 20382889]

[29]. Crawford DR, Schneider DL. Ubiquinone content and respiratory burst activity of latex-filled phagolysosomes isolated from human neutrophils and evidence for the probable involvement of a third granule. J. Biol. Chem. 1983; 258:5363–5367. [PubMed: 6304087]

[30]. Kaunitz JD, Gunther RD, Sachs G. Characterization of an electrogenic ATP and chloride-dependent proton translocating pump from rat renal medulla. J. Biol. Chem. 1985; 260:11567–11573. [PubMed: 2995342]

[31]. Hartinger J, Jahn R. An anion binding site that regulates the glutamate transporter of synaptic vesicles. J. Biol. Chem. 1993; 268:23122–23127. [PubMed: 8226829]

[32]. Tabb JS, Kish PE, Van Dyke R, Ueda T. Glutamate transport into synaptic vesicles: roles of membrane potential, pH gradient, and intravesicular pH. J. Biol. Chem. 1992; 267:15412–15418. [PubMed: 1353494]

[33]. Zoccarato F, Cavallini L, Alexandre A. The pH-sensitive dye acridine orange as a tool to monitor exocytosis/endocytosis in synaptosomes. J. Neurochem. 1999; 72:625–633. [PubMed: 9930734]

[34]. Chen X, Lee KA, Ha EM, Lee KM, Seo YY, Choi HK, Kim HN, Kim MJ, Cho CS, Lee SY, Lee WJ, Yoon J. A specific and sensitive method for detection of hypochlorous acid for the imaging of microbe-induced HOCl production. Chem. Commun. (Camb). 2011; 47:4373–4375. [PubMed: 21399827]

[35]. Simchowitz L. Interactions of bromide, iodide, and fluoride with the pathways of chloride transport and diffusion in human neutrophils. J. Gen. Physiol. 1988; 91:835–860. [PubMed: 3047312]

[36]. Gaut JP, Yeh GC, Tran HD, Byun J, Henderson JP, Richter GM, Brennan ML, Lusis AJ, Belaaouaj A, Hotchkiss RS, Heinecke JW. Neutrophils employ the myeloperoxidase system to generate antimicrobial brominating and chlorinating oxidants during sepsis. Proc. Natl. Acad. Sci. USA. 2001; 98:11961–11966. [PubMed: 11593004]

[37]. Sheppard DN, Welsh MJ. Structure and function of the CFTR chloride channel. Physiol. Rev. 1999; 79:S23–S45. [PubMed: 9922375]

[38]. Ma T, Thiagarajah JR, Yang H, Sonawane ND, Folli C, Galietta LJ, Verkman AS. Thiazolidinone, CFTR inhibitor identified by high-throughput screening blocks cholera toxin-induced intestinal fluid secretion. J. Clin. Invest. 2002; 110:1651–1658. [PubMed: 12464670]

[39]. Painter RG, Marrero L, Lombard GA, Valentine VG, Nauseef WM, Wang G. CFTR-mediated halide transport in phagosomes of human neutrophils. J. Leukocyte Biol. 2010; 87:933–942. [PubMed: 20089668]

[40]. Hara-Chikuma M, Yang B, Sonawane ND, Sasaki S, Uchida S, Verkman AS. ClC-3 chloride channels facilitate endosomal acidification and chloride accumulation. J. Biol. Chem. 2005; 280:1241–1247. [PubMed: 15504734]

[41]. Randak C, Welsh MJ. An intrinsic adenylate kinase activity regulates gating of the ABC transporter CFT. Cell. 2003; 115:837–850. [PubMed: 14697202]

[42]. Hansson MJ, Morota S, Teilum M, Mattiasson G, Uchino H, Elmer E. Increased potassium conductance of brain mitochondria induces resistance to permeability transition by enhancing matrix volume. J. Biol. Chem. 2010; 285:741–750. [PubMed: 19880514]

[43]. Griffiths EJ, Rutter GA. Mitochondrial calcium as a key regulator of mitochondrial ATP production in mammalian cells. Biochim. Biophys. Acta. 2009; 1787:1324–1333. [PubMed: 19366607]

[44]. Sturgill-Koszycki S, Schlesinger PH, Chakraborty P, Haddix PL, Collins HL, Fok AK, Allen RD, Gluck SL, Heuser J, Russell DG. Lack of acidification in Mycobacterium phagosomes produced by exclusion of the vesicular proton-ATPase. Science. 1994; 263:678–681. [PubMed: 8303277]

[45]. Lonnbro P, Nordenfelt P, Tapper H. Isolation of bacteria-containing phagosomes by magnetic selection. BMC Cell Biol. 2008; 9:35. [PubMed: 18588680]

[46]. Winterbourn CC, Hampton MB, Livesey JH, Kettle AJ. Modeling the reactions of superoxide and myeloperoxidase in the neutrophil phagosome: implications for microbial killing. J. Biol. Chem. 2006; 281:39860–39869. [PubMed: 17074761]

[47]. Segal AW, Coade SB. Kinetics of oxygen consumption by phagocytosing human neutrophils. Biochem. Biophys. Res. Commun. 1978; 84:611–617. [PubMed: 718704]

[48]. Jiang Q, Griffin DA, Barofsky DF, Hurst JK. Intraphagosomal chlorination dynamics and yields determined using unique fluorescent bacterial mimics. Chem. Res. Toxicol. 1997; 10:1080–1089. [PubMed: 9348429]

[49]. Painter RG, Wang G. Direct measurement of free chloride concentrations in the phagolysosomes of human neutrophils. Anal. Chem. 2006; 78:3133–3137. [PubMed: 16643004]

[50]. Menegazzi R, Busetto S, Dri P, Cramer R, Patriarca P. Chloride ion efflux regulates adherence, spreading, and respiratory burst of neutrophils stimulated by tumor necrosis factor-alpha (TNF) on biologic surfaces. J. Cell Biol. 1996; 135:511–522. [PubMed: 8896606]

[51]. Steinberg BE, Touret N, Vargas-Caballero M, Grinstein S. In situ measurement of the electrical potential across the phagosomal membrane using FRET and its contribution to the proton-motive force. Proc. Natl. Acad. Sci. USA. 2007; 104:9523–9528. [PubMed: 17517624]

[52]. Painter RG, Valentine VG, Lanson NA Jr, Leidal K, Zhang Q, Lombard G, Thompson C, Viswanathan A, Nauseef WM, Wang G. CFTR expression in human neutrophils and the phagolysosomal chlorination defect in cystic fibrosis. Biochemistry. 2006; 45:10260–10269. [PubMed: 16922501]

[53]. Krause KH, Welsh MJ. Voltage-dependent and Ca2(+)-activated ion channels in human neutrophils. J. Clin. Invest. 1990; 85:491–498. [PubMed: 2153708]

[54]. Moreland JG, Davis AP, Bailey G, Nauseef WM, Lamb FS. Anion channels, including ClC-3, are required for normal neutrophil oxidative function, phagocytosis, and transendothelial migration. J. Biol. Chem. 2006; 281:12277–12288. [PubMed: 16522634]

[55]. Simchowitz L, Textor JA, Vogt SK. Use of tributyltin to probe contribution of Cl^--HCO_3^- exchange to regulation of steady-state pHi in human neutrophils. Am. J. Physiol. 1991; 261:C906–C915. [PubMed: 1951675]

[56]. Stoddard JS, Steinbach JH, Simchowitz L. Whole cell Cl^- currents in human neutrophils induced by cell swelling. Am. J. Physiol. 1993; 265:C156–C165. [PubMed: 8338124]

[57]. Volk AP, Heise CK, Hougen JL, Artman CM, Volk KA, Wessels D, Soll DR, Nauseef WM, Lamb FS, Moreland JG. ClC-3 and IClswell are required for normal neutrophil chemotaxis and shape change. J. Biol. Chem. 2008; 283:34315–34326. [PubMed: 18840613]
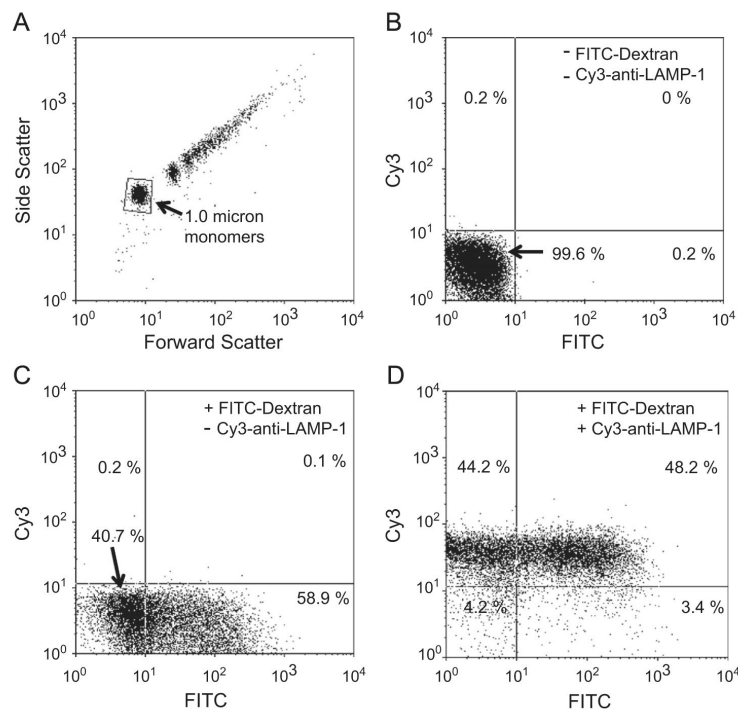
Fig. 1.
Permeability properties of magnetically isolated neutrophil phagosomes as assessed by flow cytometry. Phagosomes were isolated from human neutrophils 15 min after phagocytosis of opsonized 1-μm paramagnetic beads in the (C and D) presence or (B) absence of FITC-labeled dextran as described under Materials and methods. (D) The isolated phagosomes were stained with Cy3-conjugated rabbit anti-LAMP-1 as a marker for mature phagosomes and subjected to two-color analysis by flow cytometry. (A) The forward and side light-scatter properties of the preparation. A typical scattering pattern consisted of a monomeric fraction (arrow) and a series of higher order aggregates. Analysis of the fluorescence properties of the monomeric fraction, as gated, is shown in (B–D). (B) Phagosomes prepared in the absence of FITC–dextran and Cy3–anti-LAMP-1. Less than 0.2% of the population was positive for either marker. (C) When FITC–dextran was included in the incubation medium during particle phagocytosis, 58.9% of the phagosomes retained the FITC label after lysis and isolation. (D) When this preparation was labeled with Cy3–anti-LAMP-1 48.2% of the phagosome population was positive for LAMP-1 and FITC–dextran.
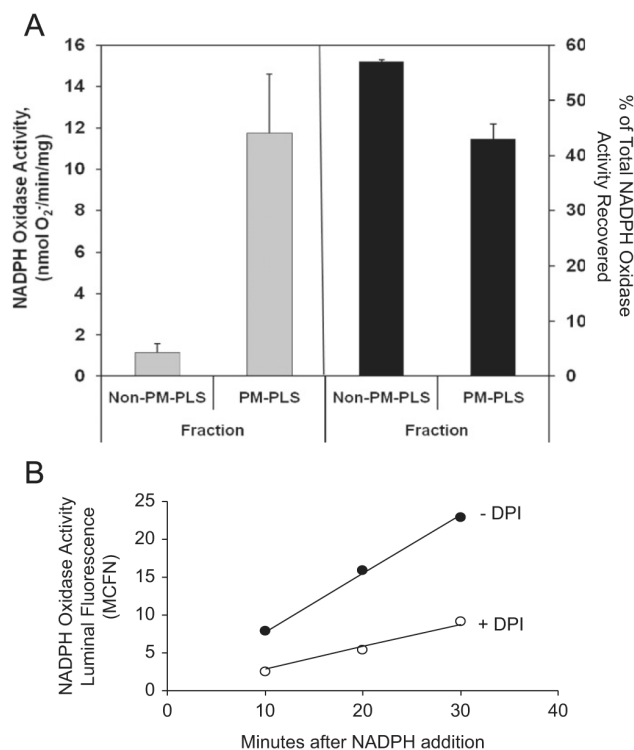
Fig. 2.
NADPH oxidase activity is enriched in the isolated phagosomal fractions. (A) Enrichment of the NADPH oxidase in the isolated phagosomes. The paramagnetic phagolysosome (PM-PLS) fraction and non-PM-PLS fraction were assayed for NADPH-oxidase activity as described under Materials and methods. The left shows the total SOD-sensitive cytochrome *c* reductase-specific enzyme activity associated with the two fractions and the right shows the percentage of total activity associated with each fraction. The PM-PLS fraction had about 40% of the total recovered activity (right) and was enriched about 12-fold relative to the non-PM-PLS fraction (left). (B) Constitutive NADPH oxidase activity in isolated phagosomes. PM-PLS were incubated in the presence of the membrane-permeative, nonfluorescent dye 5 μM dihydrorhodamine 123, in potassium gluconate relaxation buffer containing 1 mM ATP. The reaction was initiated by adding NADPH to a final concentration of 1 mM and monitoring the accumulation of green-fluorescent oxidation product in the PM-PLS monomeric fraction with time by flow cytometry. The data indicate that the oxidation of the probe was linear with time and inhibited by DPI (10 μM), indicating that the oxidation was due to the action of the NADPH oxidase.
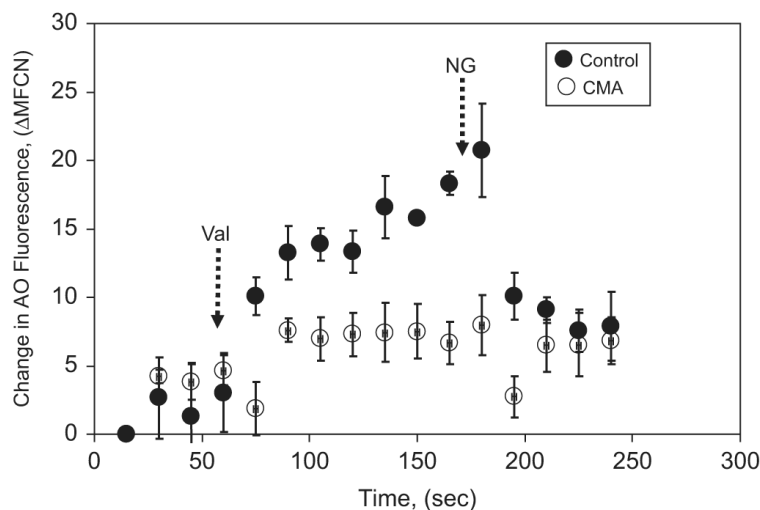
Fig. 3.
Acidification of PM-PLS as measured by acridine orange (AO) uptake by flow cytometry. The PM-PLS were prepared from neutrophils isolated with Ringer's buffer and lysed in the relaxation buffer containing protease inhibitors. Fifty microliters of the isolated PM-PLS was diluted into 0.5 ml of the chloride-rich (100 mM KCl) relaxation buffer with 1 mM ATP and 4 μM AO for 1 min and then analyzed by flow cytometry at 15-s intervals at room temperature. After the AO fluorescence associated with the monomeric particle population stabilized, valinomycin (Val; 1 μM; left dashed arrow) was added, which increased the degree of acidification over time significantly (solid circles). Addition of 7 μM nigericin (NG; right dashed arrow), which would be expected to equilibrate the PM-PLS luminal pH to the extraphagosomal pH (7.0) by exchanging extraphagosomal potassium ions for intraphagosomal protons, quenched the fluorescence associated with the PM-PLS. Inclusion of 500 nM concanamycin A (CMA) in the system blocked the valinomycin-dependent acidification response (open circles). Vertical bars represent the standard deviation of the mean of triplicate runs.
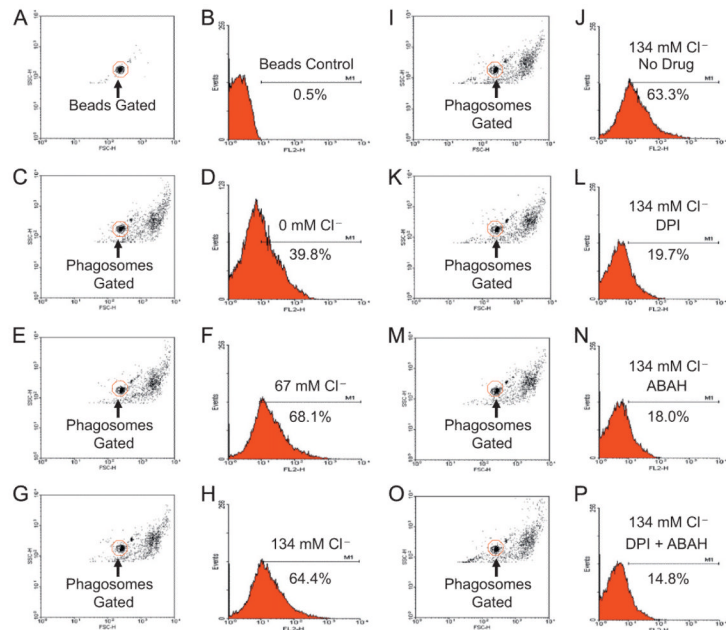
Fig. 4.
Chloride-dependent HOCl production in the isolated phagosomes. The isolated phagosomes were resuspended in the relaxation buffer with various chloride concentrations. Oxidant production was reconstituted by supplementing NADPH and detected with R19-S, a HOCl sensor. The samples were analyzed for fluorescence intensity change by flow cytometry by gating on the phagosome population. When indicated, the NADPH oxidase inhibitor DPI or the MPO inhibitor ABAH was used to validate HOCl production.
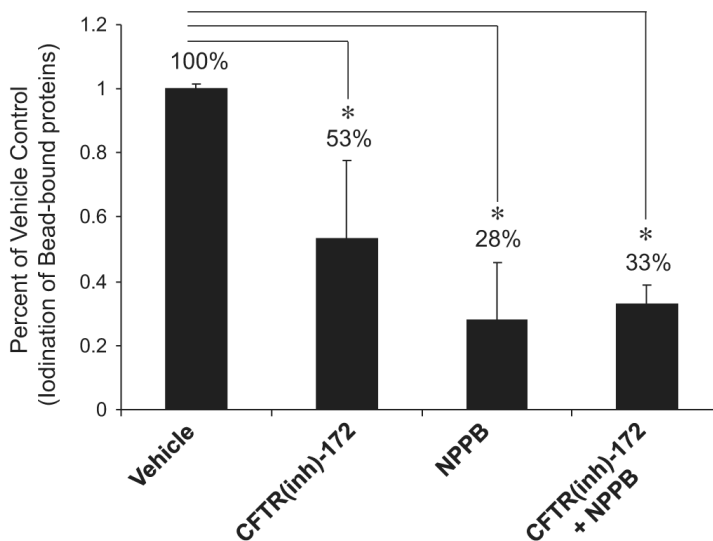
Fig. 5.
Chloride channel-mediated halide transport under active MPO oxidation. Paramagnetic phagosomes were isolated in the chloride-free relaxation buffer with 1 mM ATP. A cocktail of protease and phosphatase inhibitors was added to maintain the native structures and phosphorylation state of the phagosomal proteins. D-Methionine (10 mM) was included in the medium to scavenge any extraphagosomal HOI that may have been present. The reaction was initiated by adding hydrogen peroxide and radioiodide and allowed to proceed for 30 min at 37 °C. Drugs when present were added 10 min before initiating the reaction. The reaction was stopped by adding 3 volumes of a lysis buffer containing 0.1% Triton X-100, 100 mM KI, and 0.1% sodium metabisulfite. The detergent-extracted beads were then recovered by filtration on Millipore 0.4-μm-pored nitrocellulose filters and washed with the same buffer and radioiodine content was determined by liquid scintillation. The general anion transport inhibitor NPPB was used at a final concentration of 200 μM. CFTRinh-172 was used at 20 μM and the MPO inhibitor ABAH at 150 μM. The data are expressed as the percentage of ABAH-inhibitable iodination from each group compared to that of the vehicle control. Vertical bars represent the standard deviation of the mean. $*p<0.05$.
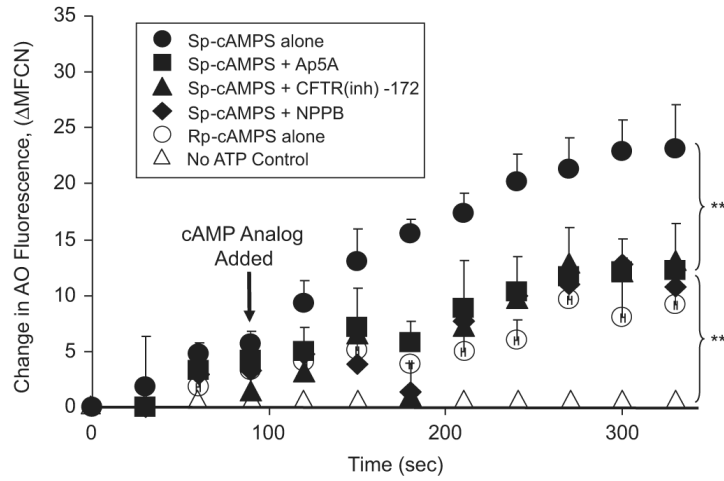
Fig. 6.
Cyclic AMP-activated acidification in isolated PM-PLS is affected by CFTR chloride channel inhibitors. The prepared PM-PLS samples were diluted into the chloride-rich 100 mM KCl relaxation buffer with or without 1 mM ATP, 4 µM AO, and various channel inhibitors for 1 min and then analyzed by flow cytometry at 15-s intervals at room temperature. Without activation of V-ATPase in the no-ATP control, no proton influx or acidification occurred. Addition of ATP and the nonhydrolyzable cAMP agonist, Sp-cAMPS (40 µM) resulted in the maximum acidification of the PM-PLS (solid circles). Inclusion of CFTR chloride channel inhibitors, Ap5A (1 mM) or CFTRinh-172 (5 µM), reduced the extent of acidification to ~54% of the maximum value at the last time point measured. NPPB, a non-CFTR chloride channel blocker (100 µM), inhibited the acidification by ~52%. The cAMP antagonist Rp-cAMPS gave rise to ~46% of the maximum acidification. All experimental data represent triplicate runs. The vertical bars represent the standard deviations from the mean. ** $p < 0.01$ by one-way ANOVA.
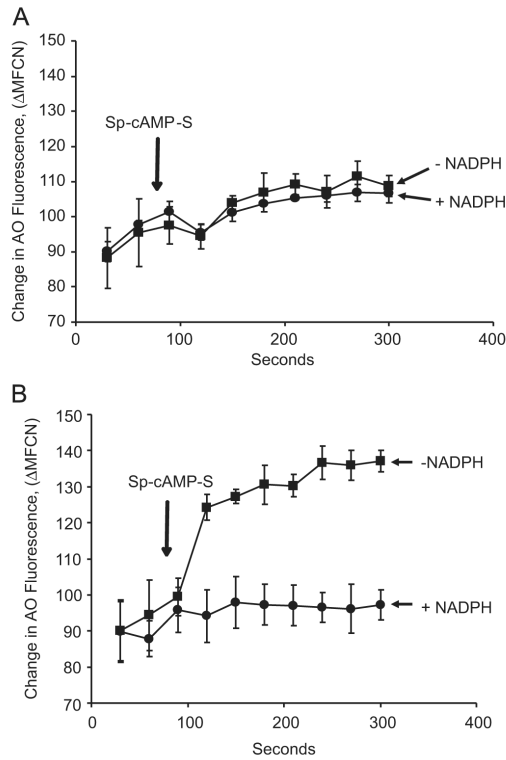
Fig. 7.
Acidification of PM-PLS is dependent on chloride, which is suppressed by an active NADPH oxidase. PM-PLS were isolated and assayed in the presence of either (A) chloride-free (K gluconate) or (B) chloride-rich (KCl) relaxation buffer containing ATP and AO, as described in the legends of Figs. 3 and 6. After establishment of a stable fluorescence baseline, Sp-cAMP-S was added as indicated by the arrow. As can be seen in (B), in the presence of extraluminal chloride rapid acidification occurred in the absence of NADPH addition but was abolished when NADPH was added to activate the oxidase. Little acidification was observed in the presence or absence of NADPH when the experiment was performed in the chloride-free medium (A).
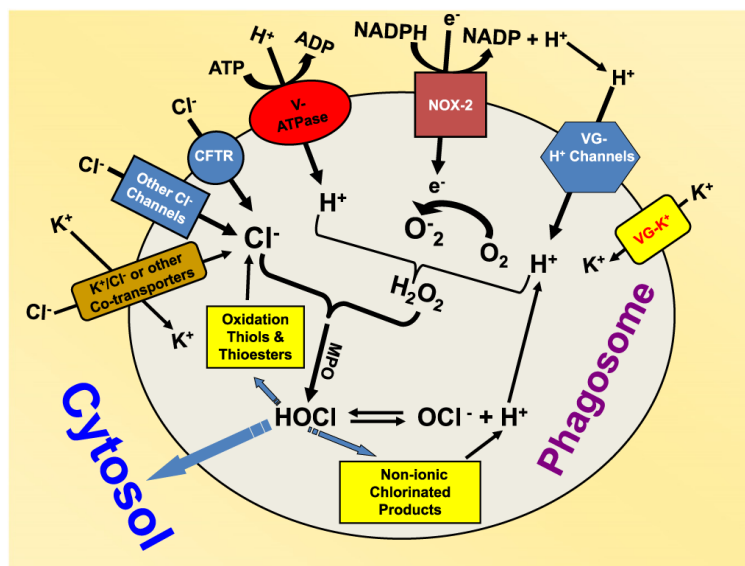
Fig. 8.
Model proposed to depict chloride intake and charge balance in neutrophil phagosomes. Oxidant production and ion dynamics are schematically displayed. The NADPH oxidase (NOX-2) is responsible for electron transport, which is balanced by cation influx through the voltage-gated proton and potassium channels. The V-ATPase-driven proton transport is balanced by chloride influx. The model suggests that phagosomes acquire chloride for HOCl production through functional association of chloride channels with the V-ATPase proton pump. VG-H$^+$ channels, voltage-gated proton channels; VG-K$^+$, voltage-gated potassium channels.

Table 1

Enrichment of protein markers in purified PM-PLS.

Fraction	Protein		LDH		MPO		LF		LAMP-1	
	Amount (mg)	%	%	Fold	%	Fold	%	Fold	%	Fold
Non-PM-PLS	12	94	99	1.0	70	0.8	5.2	0.6	16	0.2
PM-PLS	0.8	6.0	0.7	0.2	30	4.6	49	7.6	84	13

Total protein and lactate dehydrogenase (LDH) activity were measured as described under Materials and methods. Myeloperoxidase (MPO), lactoferrin (LF), and lysosomal-associated membrane protein-1 (LAMP-1) were estimated by quantitative chemiluminescence scanning of immunoblots. Fold enrichment of each marker protein is relative to the total protein recovered.